Results in Physics 6 (2016) 295–298

Contents lists available at ScienceDirect

Results in Physics

journal homepage: www.journals.elsevier.com/results-in-physics

Formation, structural and optical characterization of neodymium doped-zinc soda lime silica based glass

M.I.M. Zamratul *, A.W. Zaidan, A.M. Khamirul, M. Nurzilla, S.A. Halim

Department of Physics, Faculty of Science, Universiti Putra Malaysia, 43400 UPM Serdang, Selangor, Malaysia

ARTICLE INFO

Article history:
Received 4 April 2016
Accepted 31 May 2016
Available online 3 June 2016

Keywords:
Zinc soda lime silica glass
Nd^{3+}
Photoluminescence
UV–Vis absorption
FTIR
Optical band gap

ABSTRACT

New glass system of neodymium – doped zinc soda lime silica glass has been synthesized for the first time by melt-quenching of glass waste soda lime silica (SLS) with zinc oxide (ZnO) as precursor glass and Nd_2O_3 as dopant. In order to examine the effect of Nd^{3+} on the structural and optical properties, the prepared sample of structure $[(ZnO)_{0.5}(SLS)_{0.5}](Nd_2O_3)_x$ (x = 0, 1, 2, 3, 4 and 5 wt%) was characterized through X-ray diffraction (XRD), Fourier transform infrared (FTIR) spectroscopy, UV–Vis spectroscopy (UV–Vis) and the photoluminescence (PL). XRD pattern justifies the amorphous nature of synthesized glasses. FTIR spectroscopy has been used to observe the structural evolution of ZnO_4 and SiO_4 groups. The UV–Vis-NIR absorption spectra reveals seven peaks centered at excitation of electron from ground state $^4I_{9/2}$ to $^4D_{3/2} + {}^4D_{5/2}$ (~360 nm), $^2G_{9/2} + {}^2D_{3/2} + {}^2P_{3/2}$(~470 nm), $^2K_{13/2} + {}^4G_{7/2} + {}^4G_{9/2}$ (~523 nm), $^4G_{5/2} + {}^2G_{7/2}$ (~583 nm), $^4F_{9/2}$ (~678 nm), $^4S_{3/2} + {}^4F_{7/2}$ (~748 nm) and $^4F_{5/2} + {}^2H_{9/2}$ (~801 nm). PL spectra under the excitation of 800 nm display four emission bands centered at 531 nm, 598 nm, 637 nm and 671 nm corresponding to $^4G_{7/2} \rightarrow {}^4I_{9/2}$, ($^4G_{7/2} \rightarrow {}^4I_{11/2}$, $^4G_{5/2} \rightarrow {}^4I_{9/2}$), ($^4G_{5/2} \rightarrow {}^4I_{11/2}$) and ($^4G_{7/2} \rightarrow {}^4I_{13/2}$, $^4G_{5/2} \rightarrow {}^4I_{11/2}$) respectively.

Introduction

The need for novel environmental glass system as luminous material has urged the investigation of several possible hosts for glass doping Nd^{3+} [1–3] after decades since lasing in Nd-doped glass by Snitzer [4]. Nd^{3+} ions are often used as dopant for lasing action with high efficiency for room temperature operation. Most of the applications of Nd^{3+} ions are because it can functionalize in both amorphous and crystalline state for developing solid state lasers [5] with valuable properties of 4f shell transitions [6]. Normally, Nd is doped into glass host matrices such as borate, phosphate silicates and fluorides [7]. Among other conventional host, silicate is a promising material for Nd host glass because of its optical and mechanical features [8]. Considerable works have been reported to fabricate neodymium-doped silica glass using melt-casting [9], vapor deposition [10] and sol gel [11].

Despite that, based on the ideas of Nd doped glass, a glass – based zinc silica (ZnO-SLS) will be developed by utilizing soda lime silicate (SLS) as silica sources, zinc oxide (ZnO) and neodymium oxide (Nd_2O_3). Significance literature evidences has led to selection of SLS glass as host component [12–14]. Pioneering work has led to this project on the properties of physical, structural and optical properties of zinc soda lime silica (ZnO-SLS) [15–17], however, no extensive investigation has been performed on structural and luminescence of Nd doped ZnO-SLS properties yet.

As a crucial advantage, synthesis of ZnO together with SLS waste glass is cost effective compared to other semiconductors [18] due to its potential in optoelectronics particularly ultraviolet emitting devices [19]. In fact, the combination of rare earth ions with a wide band gap semiconductor is considered as a new class of material. In this work, a detailed yet revealing study of the structural, luminescence and optical of $(ZnO)_{0.5}(SLS)_{0.5}$ glass and Nd^{3+} doped $[(ZnO)_{0.5}(SLS)_{0.5}]$ is reported.

Experimental

The starting material was soda lime silica glass, commercial ZnO powder (Sigma Aldrich, 99.9%) and Nd_2O_3 powder (Alfa Aesar, 99.9%). The precursor glasses with composition in weight% of $[(ZnO)_{0.5}(SLS)_{0.5}]$ $(Nd_2O_3)_x$ (x = 0, 1, 2, 3, 4 and 5 wt%) were prepared by using melt-quenching in water method. For each batch, starting material of 30 g were ball milled together at 300 rpm for 48 h until fully mixed and melted in alumina crucible at 1400 °C for 2 h. The glassy frit produced was finely ground and sieved into 63 μm in size. The powdered glass was cast into pellet form of 10 mm diameter mold. The amorphous phases of powders were

* Corresponding author.

http://dx.doi.org/10.1016/j.rinp.2016.05.014
2211-3797/

evaluated by X-ray diffraction diffractometer (XRD; X'pert X-ray Diffractometer, Phillips) using with Cu K_α radiation. The samples were scanned between $(2\theta) = 4°$ and the end of angle was 90°. Analysis by infrared spectrometer in the region 400–4000 cm^{-1} was recorded for all the samples using Fourier transform infrared spectroscopy (FTIR; Perkin Elmer). UV–Visible spectra for samples were then measured by using UV–Vis spectrophotometer (UV–Vis; UV–Vis-NIR, Shimadzu). The photoluminescence spectra were measured by using Photoluminescence spectrophotometer (PL; LS 55, Perkin Elmer).

Results and discussion

XRD analysis

Fig. 1 shows the X-ray diffraction pattern of the undoped and Nd doped glass samples. Both the investigated undoped and Nd doped glass samples show neither sharp peak nor crystalline pattern. The broad peak centered at 31.9° clearly indicated that the glass samples are fully amorphous.

FTIR spectral analysis

The infrared spectra of amorphous undoped $(ZnO)_{0.5}(SLS)_{0.5}$ and $(Nd_2O_3)_x$ $[(SLS)_{0.5}(ZnO)_{0.5}]$ at room temperature are shown in Fig. 2. The vibration frequencies at 460 cm^{-1} region of the infrared spectrum is due to bending mode vibrations of O–Si–O [17,20] and Si–O–Si [17]. The vibration frequencies at 750–770 cm^{-1} region confirmed the presence of Si–O–Zn bonds which indicates the possibility of existed network formation between ZnO_4 and ZnO_3 group in precursor host [17]. A peak at 654 cm^{-1} indicates the presence of Si–O–Nd [21]. The peak observed at approximately 700–820 cm^{-1} is assumed to be related to symmetric Si–O–Si stretching or vibrational of ring structures [20] and bridging oxygen between tetrahedra [17]. The region at approximately 980 cm^{-1} explains the formation of asymmetric SiO_4 [17,22]. The peak at 1180 cm^{-1} explained the position of Si–O–Si, TO and LO asymmetric stretching bonding [20]. The absorption band at 1638 cm^{-1} indicates C=C stretching. This band is expected to vanish in dense glass [20].

UV–Vis absorption

Fig. 3 displays the UV–Vis absorption spectra of undoped and Nd doped glasses with different Nd^{3+} concentrations at room temperature. The UV–Vis absorption spectra of the undoped and Nd doped glass powders were recorded in the range of 200–800 nm.

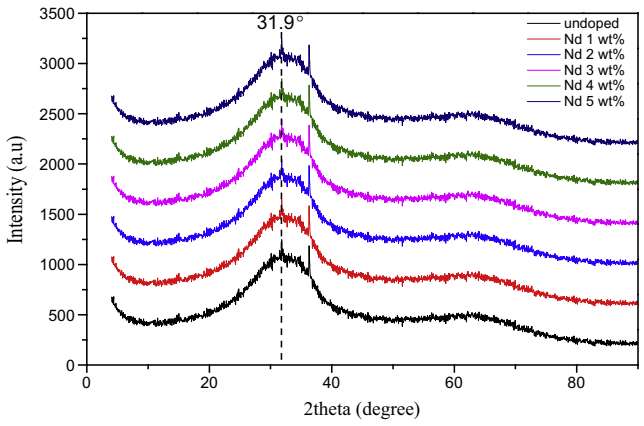

Fig. 1. XRD pattern of $[(ZnO)_{0.5}(SLS)_{0.5}](Nd_2O_3)_x$.

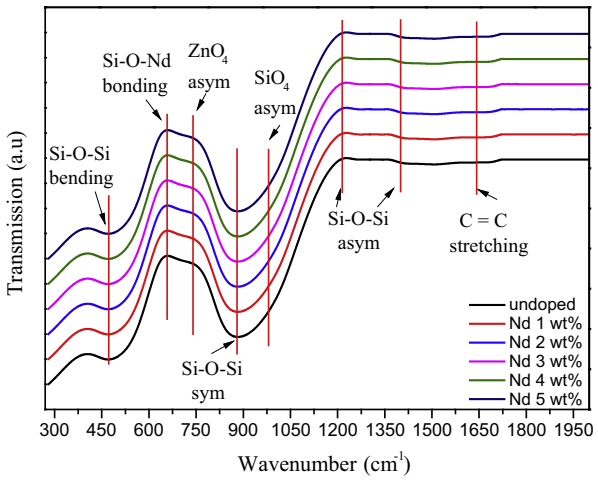

Fig. 2. FTIR evolution of $[(ZnO)_{0.5}(SLS)_{0.5}](Nd_2O_3)_x$.

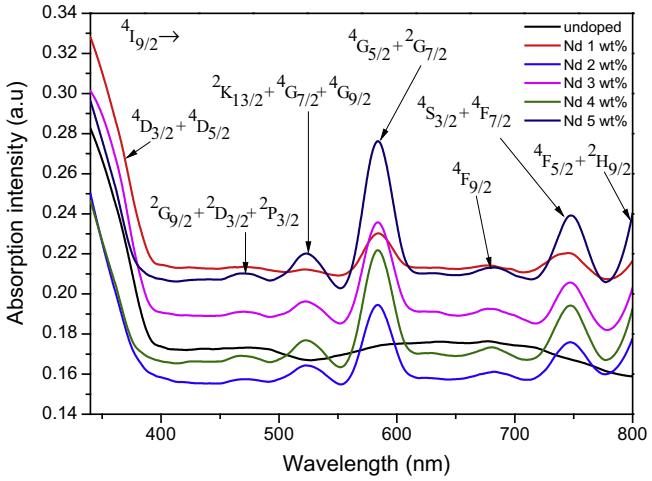

Fig. 3. UV–Vis absorption of $[(ZnO)_{0.5}(SLS)_{0.5}](Nd_2O_3)_x$.

All the doped glass samples absorption lines are due to $4f^3$–$4f^3$ transition of the Nd^{3+} ions.

The UV–Vis absorption peaks exist when the f orbital of Nd^{3+} has interaction with the neighboring O^{2-} ions. The sharpness of the peaks is due to f–f transition of the increasing Nd^{3+} doping. While no features are observed for the undoped glass sample, the Nd doped powder spectra exhibit Nd related absorption peaks at 360 nm, 470 nm, 523 nm, 583 nm, 678 nm, 748 nm and 801 nm. This phenomenon occurs as Nd^{3+} enter the lattice of ZnO-SLS, the f orbital is split into the ground and various excited energy levels. All these peaks correspond to excitation of electrons from the ground state $^4I_{9/2}$ to $^4D_{3/2} + {}^4D_{5/2}$ (~360 nm), $^2G_{9/2} + {}^2D_{3/2} + {}^2P_{3/2}$ (~470 nm), $^2K_{13/2} + {}^4G_{7/2} + {}^4G_{9/2}$ (~523 nm), $^4G_{5/2} + {}^2G_{7/2}$ (~583 nm), $^4F_{9/2}$ (~678 nm), $^4S_{3/2} + {}^4F_{7/2}$ (~748 nm) and $^4F_{5/2} + {}^2H_{9/2}$ (~801 nm).

Furthermore, for Nd^{3+} ion, $^4I_{9/2} \rightarrow {}^4G_{5/2} + {}^2G_{7/2}$ is the hypersensitive transition. It confirms the selection rule $\Delta S = 0$, $\Delta J \leqslant 2$, $\Delta L \leqslant 2$ by displaying an intense absorption peak. The intensity of the hypersensitive transition is due to ion-ligand bonding environment [23] and the covalency of Nd–O bond [24].

Optical absorption

The optical absorption of both undoped and Nd doped glass samples was characterized by UV–Vis absorbance measurements

to confirm the optical band gap energy (E_{opt}) of the samples. From the UV–Visible results, Tauc plots are drawn by using the equation suggested by Mott and Davis relation for E_{opt} [25]:

$$\alpha(\nu) = B(h\nu - E_{opt})^n / h\nu \quad (1)$$

where α is the absorption coefficient as a function of photon energy, E_{opt} is the optical band gap, B is a band tailing parameter constant and n is an index that can be obtained to assume types of transition.

$$(\alpha h\nu)^{1/2} = B(h\nu - E_{opt}) \quad (2)$$

The band gap is fitted by extrapolating the linear region of the plot $(\alpha h\nu)^{1/2}$ versus hν. As shown in Fig. 4, the bandgap for undoped $(ZnO)_{0.5}(SLS)_{0.5}$ and $[(ZnO)_{0.5}(SLS)_{0.5}](Nd_2O_3)_x$ glass samples are 3.02, 2.92, 3.03, 3.00, 3.05 and 3.04 eV respectively.

At first, the band gap decreases from undoped up to doped sample of 1 wt% Nd. Such a reduction is due to generation of non-bridging oxygen and bonding defect from replacement of Zn^{2+} with Nd^{3+}. This results in broadening of band tailing or impurity band and finally reaches and merges with the bottom of the conduction band. At 2 wt% the band gap then increases due to an increase in carrier density of the host. The increase in band gap can be understood by the Burstein–Moss effect. However, at 3 wt% the band gap decreases because carrier density of the host is saturated due to excess Nd doping. At this concentration, Nd acts as carrier traps instead of electron donors [26,27]. Furthermore, it should be noted that at very high carrier densities, due to 4 wt% and 5 wt% doping, for material with semiconductor nature (ZnO), the electron and electron-impurity scattering could cause the band gap narrowing and widening effect. The first part comes from the electron-impurity interaction. The second part arises from the columbic interaction between the carriers and results in the band gap shift [28–30].

Photoluminescence

Fig. 5 shows the PL emission of Nd doped glass samples with different doping concentrations measured at room temperature. The PL spectrum was measured under an excitation wavelength of 800 nm. It is interesting to note that, four emission bands were centered at 531 nm, 598 nm, 637 nm and 671 nm corresponding to $^4G_{7/2} \rightarrow {}^4I_{9/2}$, ($^4G_{7/2} \rightarrow {}^4I_{11/2}$, $^4G_{5/2} \rightarrow {}^4I_{9/2}$), ($^4G_{5/2} \rightarrow {}^4I_{11/2}$) and ($^4G_{7/2} \rightarrow {}^4I_{13/2}$, $^4G_{5/2} \rightarrow {}^4I_{11/2}$) respectively. The results are confirmed with previous studies on telluride optical properties [5] and PbO–GeO_2 glass [31] and lithium magnesium borate glass [1].

As shown, the emission intensity can be tremendously enhanced with the increasing Nd^{3+} doping concentration in the $[(ZnO)_{0.5}(SLS)_{0.5}](Nd_2O_3)_x$ glass samples up to 3 wt% Nd doping and quenches afterward. The quenching in the luminescence intensity is due to Nd cluster in SiO_2 matrix [32], decreasing distance in Nd^{3+} and Zn^{2+} and the promotion of multi-phonon relaxation [1].

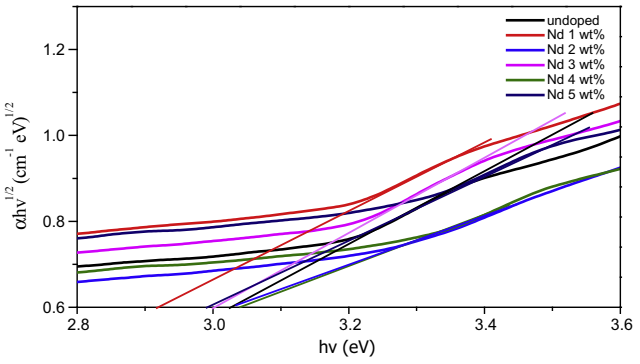

Fig. 4. Plot of $(\alpha h\nu)^{1/2}$ versus hν for $[(ZnO)_{0.5}(SLS)_{0.5}](Nd_2O_3)_x$.

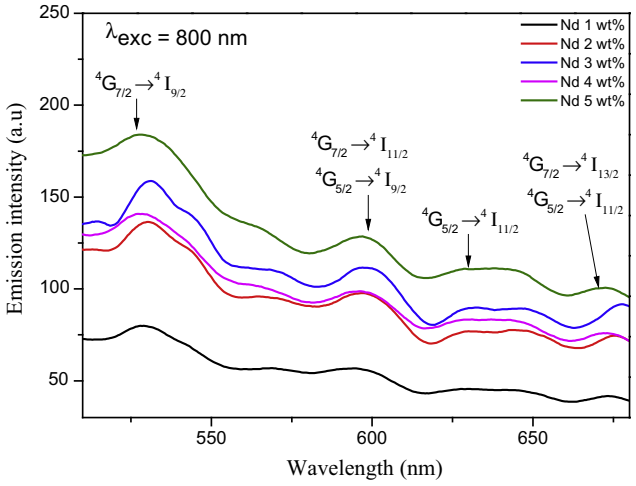

Fig. 5. PL emission (λ_{exc} = 800 nm) of $[(ZnO)_{0.5}(SLS)_{0.5}](Nd_2O_3)_x$.

Conclusions

Neodymium doped zinc soda lime silica of structure $[(ZnO)_{0.5}(SLS)_{0.5}](Nd_2O_3)_x$ (x = 0, 1, 2, 3, 4 and 5 wt%) glasses have been synthesized successfully by using melt-quenching technique. From characterization studies, XRD measurements indicate the amorphous phase of both undoped and doped glasses. FTIR measurements indicate the presence of main structural of the host material, ZnO_4 and SiO_4 groups. UV–Vis absorption shows seven bands absorption peaks related to the presence of Nd^{3+}. The increases and decreases of optical band gap are due to structural amendment, Burstein–Moss effect and band gap narrowing and widening effect. The PL spectra display distinctive red, orange and green emission with potential upconversion ability related to telecommunication and solid state lasers.

Acknowledgments

The authors would like to acknowledge Universiti Putra Malaysia for providing financial assistance through *Inisiatif Putra Berkumpulan* (IPB) research grant (IPB/2013/9412602).

References

[1] Mhareb MHA, Hashim S, Ghoshal SK, Alajerami YSM, Saleh MA, Dawaud RS, Razak NAB, Azizan SAB. Opt Mater 2014;37:391.
[2] Vázquez GV, Muñoz HG, Camarillo I, Falcony C, Caldiño U, Lira A. Opt Mater 2014;46:97.
[3] Kashif I, Abd El-Maboud A, Ratep A. Results Phys 2014;4(1).
[4] Snitzer E. Phys Rev Lett 1961;7:444.
[5] Sobczyk M. J Quant Spectr Radiat Trans 2013;119:128.
[6] Coffa S, Franzò G, Priolo F, Polman A, Serna R. Phys Rev B Condens Matter Mater Phys 1994;49:16313.
[7] Pope EJA, Mackenzie JD. J Am Ceram Soc 1993;76:1325.
[8] Qiao Y, Da N, Mingying P, Lyun Y, Danping C, Jianrong Q, Chongsan Z, Akai T. J Rare Earth 2006;24:765.
[9] Weber MJ. J Non-Cryst Solids 1990;123:208.
[10] Mears RJ. Electron Lett 1985;21:738.
[11] Chakrabati S, Sahu J, Chakraborty M, Acharya HN. J Non-Cryst Solids 1994;180:96.
[12] Mi-tang W, Jin-shu C, Mei L, Feng H. Phys B 2011;406:187.
[13] Sharma YK, Surana SSL, Singh RK. J Rare Earth 2009;27:773.
[14] Chimalawong P, Kaewkhao J, Kedkaew C, Limsuwan P. J Phys Chem Solids 2010;71:965.
[15] Matori KA, Zaid MHM, Sidek HAA, Halimah MK, Wahab ZA, Sabri MGM. Int J Phys Sci 2010;5:2212.

[16] Zaid MHM, Matori KA, Sidek HAA, Halimah MK, Azmi BZ, Sabri MGM. Int J Mol Sci 2012;13:7550.
[17] Zaid MHM, Matori KA, Quah HJ, Lim WF, Sidek HAA, Halimah MK, Yunus WMM, Wahab ZA. J Mater Sci 2015;26:3722.
[18] Chakradhar RPS, Nagabhushana BM, Chandrappa GT, Ramesh KP, Rao JL. J Chem Phys 2004;121:10250.
[19] Jannoti A, Van de Walle CG. Phys Rev B 2007;76:165202.
[20] Wang SS, Zhou Y, Lam YL, Kam CH, Chan YC, Yao X. Mat Res Innovat 1997;1:92.
[21] Duhan S, Aghamkar P. Research Lett Phys 2008:237023.
[22] Ramakrishna PV, Murthy DBRK, Sastry DL. Spectrochem Acta Part A Mol Biomol Spectrosc 2014;125:234.
[23] Pascuta P, Pop L, Rada S, Bosca M, Culea E. J Mater Sci: Mater Electron 2008;19:424.
[24] Ratnakaram YC, Vijaya kumar A, Thirupathi Naidu D, Chakradhar RPS, Ramesh KP. J Lumin 2004;110:65.
[25] Mott NF, Davis EA. Electronic processes in non-crystalline materials. UK: Clarendon Press; 1971.
[26] Weijten CHL, Van Loon PAC. Thin Solid Films 1992;196:1.
[27] Gupta L, Mansingh A, Srivastava PK. Appl Surf Sci 1988;33(34):898.
[28] Dakhel AA. J Alloys Comp 2009;475:51.
[29] Dakhel AA. Sol Energy 2009;83:934.
[30] Dakhel AA. Chem Phys 2011;130:398.
[31] da Silva DS, de Assumpcao TAA, Kassab LRP, De Araújo CB. J Alloy Comp 2014;586:S516.
[32] Moreshead WV, Nogues R, Krabill RH. J Non-Cryst Solids 1990;121:267.